Thermodynamic Characteristics of Chain Molecules in the Nematic State: *PVT* Studies of Main-Chain Liquid Crystal Comprising a Long Oxyethylene-Type Spacer

Akihiro Abe,*,† Toshihiro Hiejima,† Yoshinori Kobayashi,† Zhiping Zhou,†,§ and Chitoshi Nakafuku‡

Department of Applied Chemistry, Tokyo Polytechnic University, 1583 Iiyama, Atsugi 243-0297, Japan, and Faculty of Education, Kochi University, Kochi 780-8520, Japan

Received October 24, 2006; Revised Manuscript Received November 29, 2006

ABSTRACT: Thermodynamic characteristics of a dimer liquid crystal comprising a relatively long spacer $-O(CH_2CH_2O)_6-$ were investigated. The contour length of the flexible spacer (∼25 Å) exceeds that of the hard segments (∼18 Å). The compound exhibits a nematic mesophase (N) between the crystal (C) and the isotropic melt (I) over a sizably wide temperature range (∼80 °C). Thermodynamic quantities such as thermal expansion coefficient α, isothermal compressibility β, thermal pressure coefficient γ ($=\alpha/\beta$), and the volume change ΔV at the CN and NI interphase were carefully determined by the *PVT* measurements. The transition entropies due to volume expansion were estimated by the well-known relation $\Delta S_V = \gamma \Delta V$. The latent entropies $(\Delta S_{tr})_P$ for both CN and NI transitions were estimated according to the Clapeyron relation from the *PVT* and DTA data. The magnitude of the constant-volume entropy changes $(\Delta S_{tr})_V$ calculated was found to be about 50−60% of the corresponding values of $(\Delta S_{tr})_P$. These results were consistent with the previous ^{2}H NMR observations that the chain segments adopt a nematic conformation in the LC state. The thermodynamic role of the flexible segment in determining the phase transitions has been critically discussed.

1. Introduction

In a series of papers,[1] we have reported the structure−property relation of segmented chain molecules comprising mesogenic units jointed by intervening flexible spacers. One of the most important features of these compounds is their ability to form a mesophase between the crystalline (C) and the isotropic (I) molten state. Both boundaries are clearly defined by the first-order phase transitions. When the neighboring mesogenic cores are separated by a long flexible spacer, the liquid crystalline (LC) phase formed is often nematic (N). In such a partially ordered state, long chain segments exhibit some characteristic conformational ordering.

Since the degree of polymerization (DP) dependence of physical properties is expected to be most distinct in the oligomer region,[2] a homologous series of dimer (also called a twin compound), trimer, and polymer LCs having α,ω-dialkoxyalkane spacers were carefully examined in our previous work. Efforts were made to elucidate the conformational ordering of the spacer[4] by using various methods such as ^{2}H NMR (quadrupolar splitting),[5−9] SQUID (anisotropy of the magnetic susceptibility),[10,11] and ^{13}C NMR (^{13}C chemical shift tensor, ^{13}C−^{13}C dipolar coupling).[12,13] Studies were further extended to include the effect of the size and orientation of mesogenic units,[14] the effect due to the disorientation (tilting angle) at the junction jointing the mesogenic unit with the spacer,[15] and the optical anisotropy of the partially ordered spacer and its contribution to the orientation-dependent attractive interactions.[16] The main emphasis was placed on the thermodynamics involved in the formation of the LC state of the main-chain LC compounds.[1] In these studies, the conformational entropies calculated from the spectroscopic observations were shown to be favorably compared with the constant-volume transition entropies estimated from the *PVT* analysis.[17−21] Accumulation of various evidence suggests that the spatial configuration of the flexible spacer and its thermodynamic role remain nearly identical independent of DP from dimer to polymers.[1]

Through these studies, we have found that upon cooling from the isotropic phase the spatial arrangements which are incompatible with the nematic potential field are suppressed at the phase boundary, leaving a group of well-defined configurations in the nematic LC state. Consequently, the flexible spacer assumes more or less extended conformation in the LC state. Since this is a newly found group of spatial arrangements of chain molecules, they are termed the nematic conformation.[1] While the orientational fluctuation of the entire molecule varies as a function of temperature, the nematic conformation of the spacer remains nearly invariant over the entire range of the LC state.

The most popular chain segment used as a spacer is either *n*-alkane or oxyethylene type. The lowest energy state of the former is the all-trans planar arrangement, which can be readily accommodated in the nematic environment. In contrast, polyoxyethylene (POE) is known as one of the most flexible polymers, and the chain normally crystallizes in a 7/2 helical arrangement.[22] The OC−CO moiety of the POE chain prefers to take a gauche form in an unconstrained state.[23] Elucidation of the nematic conformation of the oxyethylene spacer $-(OCH_2CH_2)_x-$ ($x = 2, 3$) has been attempted.[24] More recently, the preparation and the preliminary results of spectroscopic studies of dimer LCs (called MBBE-x with $x = 2-6$) have been reported.[25] The phase transition temperatures of MBBE-x ($x = 2-9$) have been determined by DSC and are indicated in Chart 1.[26] The number of atoms involved in the spacer increases in

† Tokyo Polytechnic University.
‡ Kochi University.
§ Present address: School of Materials Science and Engineering, Jiangsu University, 301 Xuefu Road, Zhenjiang, Jiangsu Province 212013, China.
* Corresponding author. E-mail: aabe@chem.t-kougei.ac.jp.

10.1021/ma062447j CCC: $37.00
Published on Web 02/08/2007

Chart 1

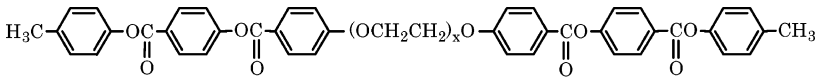

MBBE-x (x = 2 ~ 9)

x = 2:	C	191.8	N	301.5	I (°C)
x = 3:	C	165.4	N	283.4	I (°C)
x = 4:	C	148.0	N	242.9	I (°C)
x = 5:	C	132.2	N	216.1	I (°C)
x = 6:	C	106.6	N	189.8	I (°C)
x = 7:	C	94.5	N	147.2	I (°C)
x = 8:	C	91.0	N	128.4	I (°C)
x = 9:	C	88.8	N	115.5	I (°C)

Chart 2

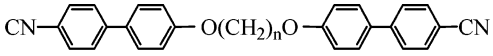

α,ω-Bis(4-cyanobiphenyl-4'-yloxy)alkanes (CBA-n)

n = 9:	C	134.8	N	173.0	I (°C)
n = 10:	C	164.6	N	184.0	I (°C)

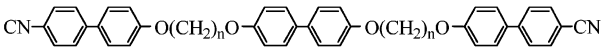

4,4'-Bis[ω-(4-cyanobiphenyl-4'-yloxy)alkoxy]biphenyls (CBA-Tn)

n = 9:	C	146.0	N	195.7	I (°C)
n = 10:	C	188.5	N	209.9	I (°C)

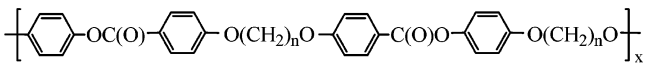

Mainchain polymer LCs with α,ω-dialkoxyalkane spacers

n = 9:	C	140	N	200	I (°C)
n = 10:	C	169	N	204	I (°C)

the order according to the series $3x - 1$. Transition temperatures and latent heats do not exhibit any appreciable odd−even oscillation when plotted against *x*.

In the present work, we wish to report *PVT* characteristics of MBBE-6 which includes a relatively long spacer derived from hexa(ethylene glycol). The contour length of the flexible spacer (~25 Å) exceeds that of the hard segments (~18 Å). The compound exhibits an interstitial N phase between C and I over a sizably wide temperature range (~80 °C), thus most suited for the reliable estimates of thermodynamic properties of the LC state. The results will be compared with those previously reported for the dimer and trimer compounds as well as polymers with α,*ω*-dialkoxyalkane spacers such as those shown in Chart 2. All of the compounds listed exhibit stepwise crystallization via a nematic state. The effect of the intervening nematic conformation on the crystallization process has been discussed in our recent review article,[1] where a part of the results obtained for MBBE-6 have been included. The details of the experimental procedure and the results of the analysis on MBBE-6 are here reported for the first time.

The *PVT* studies were also attempted for MBBE-5.[26] A reliable estimate of thermodynamic data was however hampered by the limited temperature range (~30 °C) of the stable isotropic state, and thus the results are not included.

2. Samples and Measurements

The preparation of MBBE-6 has been described previously.[25,26] The phase transition temperatures observed by using a DSC (TA Instruments Inc. model 2920) are given to the chemical formula shown in the Introduction. Orientational characteristics of the sample in the LC state were investigated by the ^{2}H NMR method, and the variation of the order parameter with temperature has already been reported.[25,26]

A *PVT* apparatus manufactured by GNOMIX Co. was used to determine the change in specific volume as a function of temperature and pressure. Measurements were carried out in the isothermal mode; volume readings were recorded over a pressure range from 10 to 100 MPa at a fixed interval (10 MPa) while the temperature was kept invariant. The temperature was then changed by 10 °C and the process repeated. In the standard measurement, a sample of 0.8 g was used. Prior to the *PVT* measurements, the density of the sample was determined with a pycnometer (volume ca. 10 mL) at 25 °C under atmospheric pressure. Calibration was carried out by using reagent grade ethanol. The density was thus found to be $d^{21} = 1.26$ g cm^{-3}.

Following our previous treatment on CBA-*n* and CBA-T*n*,[19,21] the thermal behaviors were also examined under hydrostatic pressures up to 200 MPa by using a high-pressure differential thermal analysis (DTA) apparatus. The sample covered by aluminum foil was fixed onto an alumel−chromel thermocouple junction by giving it a coating with an epoxy adhesive, which at the same time prevented the sample from direct exposure to the pressure fluid (silicone oil). The temperature and the heat of transition were calibrated with an indium standard at given pressures: the accuracy of the observed enthalpy of transition is estimated to be ±10%. The DTA measurements were performed by using 5−7 mg samples at a scanning rate of 5 deg min^{-1} under given hydrostatic pressures. Transition temperatures were defined at the maxima of the exo- and endothermic peaks in these DTA measurements.

3. Analytical Procedure of the *PVT* Data

Following our previous treatment,[17,20] we have attempted to elucidate the magnitude of the constant-volume transition entropy $(\Delta S_{tr})_V$ at both CN and NI phase boundaries under atmospheric pressure. (Hereafter the subscript tr represents a transition at the crystal−nematic (CN) or nematic−isotropic (NI) interphase.) For this purpose, the transition entropies observed under constant pressure must be corrected for the volume change

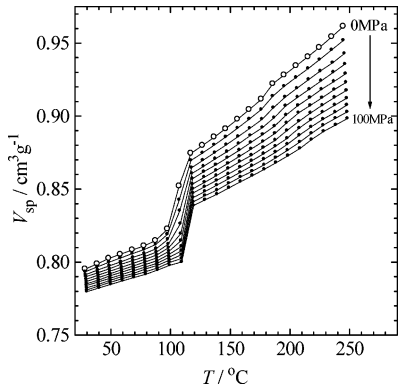

Figure 1. Volume vs temperature relations for MBBE-6 from 10 to 100 MPa. The uppermost curve (open circles) indicates the extrapolated values to zero pressure.

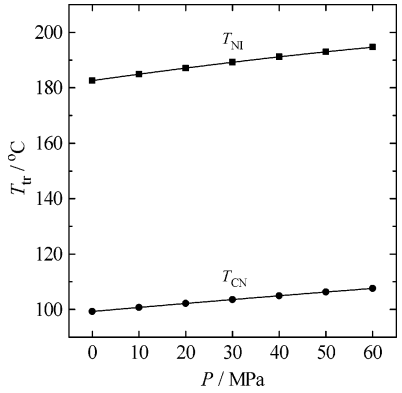

Figure 2. Variation of phase transition temperatures T_{CN} (circles) and T_{NI} (squares) as a function of pressure derived from the *PVT* data.

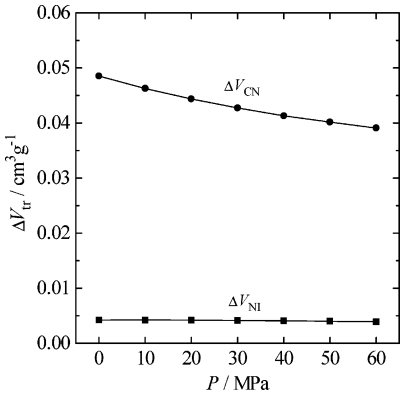

Figure 3. Variation of transition volumes ΔV_{CN} (circles) and ΔV_{NI} (squares) as a function of pressure.

ΔV_{tr}. According to Mandelkern's book,[27,28] the volume-correction term ΔS_V is defined as

$$\Delta S_V = \gamma \Delta V_{tr} = (\alpha/\beta)\Delta V_{tr} \quad (1)$$

where γ ($=\alpha/\beta$) is the thermal pressure coefficient at the transition, α the thermal expansion coefficient at constant pressure, and β the compressibility at constant temperature. In this hypothetical entropy-separation process, the physical meaning of the γ value estimated at the transition point has been controversial in the literature.[29−37] In the present analysis, we have examined this subject in some detail (see the following).

We have learned from our experience that the estimation of the transition entropy by DSC often leads to somewhat inconsistent results. Following our previous arguments on

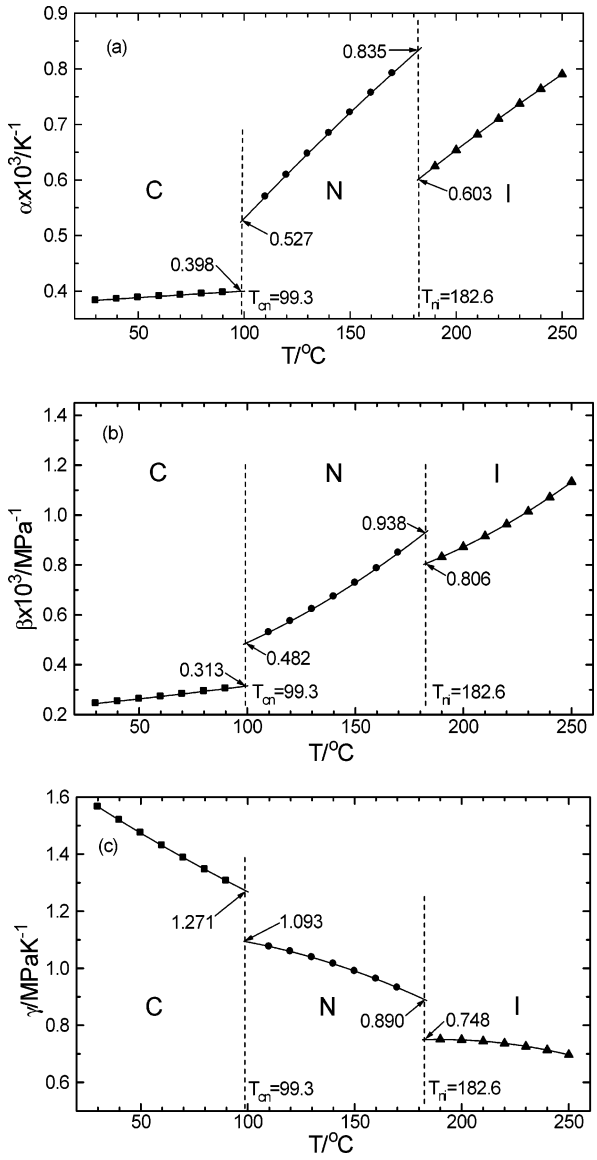

Figure 4. (a) Thermal expansion coefficient α, (b) isothermal compressibility β, and (c) thermal pressure coefficient γ ($=\alpha/\beta$) as a function of temperature. The CN and NI transition temperatures at an ordinary pressure are indicated by dotted lines. The numerical values of γ shown in (c) are those used in the present calculation (see text).

CBA-*n* and CBA-T*n*,[17,20] the $(\Delta S_{tr})_P$ values were thus estimated by using the Clapeyron relation:

$$\Delta S_{tr} = \Delta H_{tr}/T_{tr} = \Delta V_{tr}(dp/dt)_{tr} \quad (2)$$

where $(dp/dt)_{tr}$ designates the slope of the phase boundary curve in the low-pressure region. Since the reliable estimation of $(\Delta S_{tr})_P$ is crucially important, the temperature dependence of the phase boundary curve $(dp/dt)_{tr}$ was determined in two ways: one directly from the *PVT* data and the other by employing the DTA method on the same sample.

4. Results

4.1. Estimation of ΔV_{tr}, γ_{tr}, and ΔS_V on the Basis of *PVT* Measurements. The $V-T$ measurements were performed in the isothermal mode by raising temperature up to 250 °C. An example of the diagram is shown in Figure 1. The specific volumes at zero pressure ($p = 0$) were estimated from those observed at higher pressures: extrapolations were executed by using polynomial expressions. The extrapolated values are

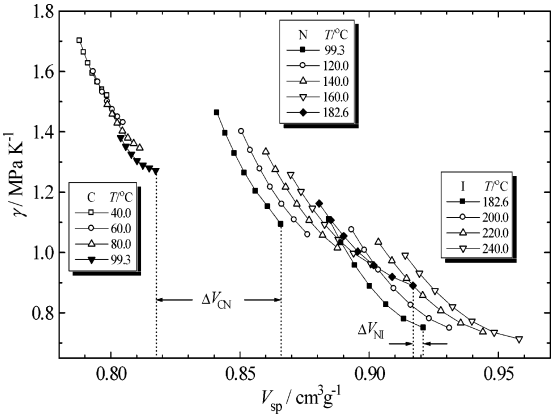

Figure 5. Variation of thermal pressure coefficient γ as a function of specific volume v_{sp} at given temperatures, obtained from the analysis of *PVT* data in each phase. The γ values corresponding to the transition temperature were estimated by exptrapolation. The incidences of the phase transition (ΔV_{CN} and ΔV_{NI}) are indicated by dotted lines.

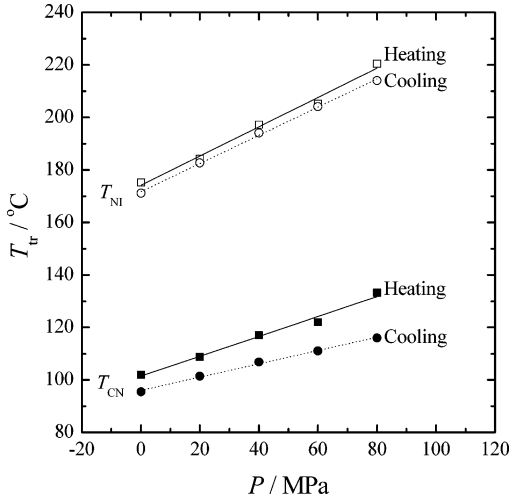

Figure 6. Variation of phase transition temperatures T_{CN} (filled) and T_{NI} (open) as a function of pressure determined by DTA (cf. Figure 2).

indicated by open circles in the diagram. A visual examination after completion of the heating measurement indicates that the sample may be to some extent degraded at higher temperatures ~250 °C. Slight deviations of the plot from the strictly vertical line at fixed temperatures are observed in Figure 1. Some small systematic drift (~2 °C over a 90 MPa span) seems to be inherent to the apparatus.[38] The analysis was carried out according to the *PVT* data numerically recorded.

The melting point T_{CN} and the isotropization temperatures T_{NI} may be in principle defined as the midpoint of the corresponding transitions indicated in the $V-T$ diagram. The melting of MBBE-6 is however a moderate S-shaped process taking place over a certain temperature range (85−115 °C) with an increment of ca. 7% in volume. For the purpose of determining unambiguous values of T_{CN} and T_{NI}, the initial and final points of the melting process were estimated from the $V-T$ curve, and the midpoint defined in this manner was taken to be the transition temperature. Variations of T_{CN} and T_{NI} thus estimated are plotted against pressure in Figure 2. The volume changes ΔV_{tr} at T_{CN} and T_{NI} can be obtained from the observed $V-T$ relation. Variations of ΔV_{tr} with pressure observed during the heating process are illustrated in Figure 3. While the volume change ΔV_{CN} at the CN transition tends to be moderately depressed as pressure increases, the corresponding transition volume ΔV_{NI} at the NI interphase is relatively insensitive to pressure. The estimated values for the ordinary pressure are $\Delta V_{CN} = 45.8$ and $\Delta V_{NI} = 4.0$ cm^3 mol^{-1}.

The magnitude of α and β in the low-pressure region is the major interests in this work. The values estimated using appropriate polynomial expressions are plotted as a function of temperature in Figures 4a (α-T) and 4b (β-T), where the phase transition boundaries T_{CN} and T_{NI} are indicated by the dotted lines. In the real measurements, a pronounced anomaly usually appears in the immediate vicinity of T_{NI}. The values given in the figure are those extrapolated from the stable regions and thus unaffected by the anomaly. The thermal pressure coefficients γ were calculated from these diagrams at given temperatures and illustrated in a similar manner in Figure 4c. Conforming to the concept of eq 1 for the constant-volume transition entropies $(\Delta S_{tr})_V$, the values of γ ($= (\delta S/\delta V)_T$ are plotted against specific volume v_{sp} for given temperatures in Figure 5. In the figure, the bounds of the transition volumes ΔV_{tr} are indicated by the arrows for both T_{CN} and T_{NI}. The curves become discontinuous at the phase boundaries, giving two different estimates for the γ value defined in eq 1. The higher temperature phase gives a lower estimate of γ. The discrepancies amount to ~14 and ~8% respectively for the CN and NI transitions (cf. Figure 4). Since the molecular configurations are quite different between the two neighboring phases, the discontinuity in the first derivatives of *PVT* quantities may be taken to be natural. Such a discrepancy however immediately suggests that the values of the constant-volume transition entropy may vary depending on which imaginary route is adopted in its estimate. Use of eq 1 in calculating $(\Delta S_{tr})_V$ inevitably suffers from such ambiguity in γ's. Nonetheless, the expression is at least approximately useful in separating the transition entropy in two parts: $(\Delta S_{tr})_P = (\Delta S_{tr})_V + \Delta S_V$. In most cases, the γ values can be determined more accurately for the fluid state than in the crystalline solid state. In the present example, the two phases separated by the NI transition are both fluid state, for which the determination of the *PVT* properties can be performed relatively in high precision.

4.2. Pressure Dependence of Phase Boundary Curves and Estimation of $(\Delta S_{tr})_P$. The variation of the phase transition temperature as a function of pressure can be elucidated from the *PVT* data, as shown in Figure 2. The values thus obtained are $(dp/dt)_{CN} = 3.47$ and $(dp/dt)_{NI} = 2.25$ MPa K^{-1}.

The same physical quantities can be elucidated from the DTA curve measured under enhanced hydrostatic pressures. The samples adopted for the measurement were those prepared by crystallization under a high pressure. Upon heating, the endothermic CN phase transition exhibits double peaks in all observations, suggesting a possible coexistence of two crystalline

Table 1. Phase Transition Enthalpies and Entropies of MBBE-6

	CN transition			NI transition		
	T_{CN} (K)	ΔH_{CN} (kJ mol^{-1})	ΔS_{CN} (J mol^{-1} K^{-1})	T_{NI} (K)	ΔH_{NI} (kJ mol^{-1})	ΔS_{NI} (J mol^{-1} K^{-1})
DSC	379.8	40.0	105.4	463.0	1.3	2.9
PVT (Clapeyron)	372.4	59.2	158.9	455.7	4.1	9.0
DTA[a] (Clapeyron)	374.6	45.3	120.9	447.3	3.2	7.2

[a] Values of ΔV_{tr} required for the calculation of ΔH_{tr} and ΔS_{tr} were borrowed from the *PVT* measurements.

Table 2. Constant-Volume Transition Entropies $(\Delta S_{CN})_V$ and the Ratio to Those $(\Delta S_{CN})_P$ under Constant Pressure for Dimer and Trimer LCs at the CN Phase Transitions

	CN transition				
compound	T_{CN} (K)	ΔS_V (J mol^{-1} K^{-1})	$(\Delta S_{CN})_P$ (J mol^{-1} K^{-1})	$(\Delta S_{CN})_V$ (= $(\Delta S_{CN})_P - \Delta S_V$) (J mol^{-1} K^{-1})	$(\Delta S_{CN})_V/(\Delta S_{CN})_P$
			Dimer LCs with α,ω-Dialkoxyalkane Spacer		
CBA-9	412.2[a]	66.0	147.0,[b] 127.1[c]	81.0,[b] 61.1[c]	0,48−0.55
CBA-10	438.2 [a]	67.4	143.8,[b] 132.0[c]	76.4,[b] 64.6[c]	0.49−0.53
			Trimer LCs with α,ω-Dialkoxyalkane Spacer		
CBA-T9	419.2[d]	97.1	222.5[c]	125.4[c]	0.56
CBA-T10	461.7[d]	103.1	226.0[c]	122.9[c]	0.54
			Dimer LC with Oxyethylene Spacer		
MBBE-6	372.4[e]	49.9 (N)[e]	158.9,[e] 120.9 [f]	109.0 (N),[e], 71.0 (N)[f]	0.59−0.69
		58.2 (C)[e]		100.7 (C),[e] 62.7 (C)[f]	0.52−0.63

[a] Reference 17. [b] Reference 19. [c] Reference 21. [d] Reference 20. [e] *PVT*: the γ values used for elucidation of ΔS_V are obtained by extrapolation from either the N or C phase as indicated in parentheses. [f] The value of $(\Delta S_{CN})_P$ was estimated by DTA.

Table 3. Constant-Volume Transition Entropies $(\Delta S_{NI})_V$ and the Ratio to Those $(\Delta S_{NI})_P$ under Constant Pressure for Dimer and Trimer LCs at the Ni Phase Transitions

	NI transition				
compound	T_{NI} (K)	ΔS_V (J mol^{-1} K^{-1})	$(\Delta S_{NI})_P$ (J mol^{-1} K^{-1})	$(\Delta S_{NI})_V$ (=$(\Delta S_{NI})_P - \Delta S_V$) (J mol^{-1} K^{-1})	$(\Delta S_{NI})_V/(\Delta S_{NI})_P$
			Dimer LCs with α,ω-Dialkoxyalkane Spacer		
CBA-9	468.9[a]	7.0	14.9,[a] 15.3,[b] 13.1[c]	7.9,[a] 8.3,[b] 6.1[c]	0.47−0.54
CBA-10	466.9[a]	8.8	22.1,[a] 15.3,[b] 19.0[c]	3.3,[a] 6.5,[b] 10.2[c]	0.42−0.60
			Trimer LCs with α,ω-Dialkoxyalkane Spacer		
CBA-T9	468.9[d]	10.3	25.0,[d] 20.8[c]	14.7,[d] 10.5[c]	0.50−0.59
CBA-T10	483.1[d]	19.3	49.8,[d] 43.2[c]	30.5,[d] 23.9[c]	0.55−0.61
			Dimer LCs with Oxyethylene Spacer		
MBBE-6	455.7[e]	3.0 (I)[e]	8.98,[e] 7.16[f]	5.98 (I),[e] 4.16 (I)[f]	0.58−0.67
		3.56 (N)[e]		5.42 (N),[e] 3.60 (N)[f]	0.50−0.60

[a] Reference 17. [b] Reference 19. [c] Reference 21. [d] Reference 20. [e] *PVT*: the γ values used for elucidation of ΔS_V are obtained by extrapolation from either the I or N phase as indicated in parentheses. [f] The value of $(\Delta S_{NI})_P$ was estimated by DTA.

Table 4. Constant-Volume Transition Entropies $(\Delta S_{NI})_V$ and the Ratio to Those $(\Delta S_{NI})_P$ under Constant Pressure for Representative Monomer LCs for the Ni Phase Transitions[a]

compound	T_{NI} (K)	ΔS_V (J mol^{-1} K^{-1})	$(\Delta S_{NI})_P$ (J mol^{-1} K^{-1})	$(\Delta S_{NI})_V$ (J mol^{-1} K^{-1})	$(\Delta S_{NI})_V/(\Delta S_{NI})_P$
5CB	308.4	1.5	2.1	0.6	0.29
7CB	315.9	2.4	2.8	0.4	0.14
5OCB	340.6	1.1	1.3	0.2	0.15
8OCB	352.9	1.5	2.3	0.8	0.35

forms. The DSC analysis at an ordinary pressure indicates that the low-temperature peak merges into the higher one by a heat treatment (annealing) at temperatures between these two peaks. Variation of the Raman absorption spectra at phase transitions suggests that the conformation around the OC−CO bond changes from the gauche-rich (1156 cm^{-1}) in I and N to a mixture of the gauche (1156 cm^{-1}) and trans (1166 cm^{-1}) forms in C on cooling.[26] Under such circumstances, the high-temperature T_{CN} peaks were adopted in the following Clapeyron analysis. The phase transition peaks observed at 0.1 MPa by DTA are T_{CN} = 101.4 and T_{NI} = 174.1 °C, which are respectively lower by about 5 and 17 °C than those obtained by DSC (Table 1). The pressure dependence of the transition temperatures, T_{NI} and T_{CN}, is shown in Figure 6. The phase transition curves can be approximated by the first-order polynomial forms: $t = a + bp$ (t = temperature, p = pressure). The coefficients obtained for the heating process (solid lines) are as follows: T_{CN}/°C, a = 101.4, b = 0.379 and T_{NI}/°C, a = 174.1, b = 0.558. The values of $(dp/dt)_{tr}$ required in eq 2 are estimated to be $(dp/dt)_{CN} = 2.64$ and $(dp/dt)_{NI} = 1.79$ MPa K^{-1}. The magnitude estimated by DTA amounts to about 80% of those from the *PVT* measurement. The representative thermodynamic quantities (T_{tr}, ΔH_{tr}, and ΔS_{tr}) obtained from DSC, *PVT*, and DTA are compared in Table 1. The values of ΔH_{tr}, and ΔS_{tr} derived from DSC are substantially lower than those from the Clapeyron relation on both *PVT* and DTA data.

4.3. Elucidation of Constant-Volume Entropy Change $(\Delta S_{tr})_V$. The values of ΔS_V, $(\Delta S_{tr})_P$, and the transition entropies at constant volume $(\Delta S_{tr})_V$, defined as the difference between $(\Delta S_{tr})_P$ and ΔS_V in eq 1, are listed in Tables 2 and 3 respectively for the CN and NI transitions. For comparison, the corresponding values of CBA-*n* and CBA-T*n* are included in these tables. The values of $(\Delta S_{tr})_P$ derived from both *PVT* and DTA were accommodated. For MBBE-6, two ΔS_V values are listed: the difference is due to how the γ_{tr} values are derived (see Figure 4). Accordingly, four values of $(\Delta S_{tr})_V$ estimated via somewhat different routes are shown in the table. Given in the last column of these tables are the ranges of the ratio $(\Delta S_{tr})_V/(\Delta S_{tr})_P$, indicating the contribution of the constant-volume entropy change to the total transition entropy observed under ordinary pressure. For the dimer and trimer compounds including MBBE-6, the ratios are found to be 50−60% for both the CN and NI transitions. For the purpose at hand, the differences arising from the two alternative choices of γ for MBBE-6 are reasonably small, and the conclusions drawn are unaffected (cf. the last row of Tables 2 and 3). The prescription given by eq 1 is, despite

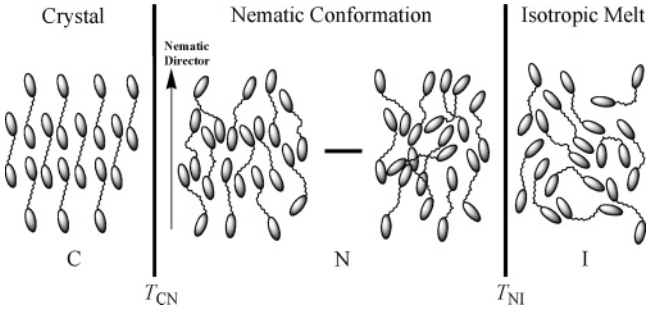

Figure 7. Schematic representation of the nematic conformation. The conformational distribution of the spacer remains quite stable in the nematic region defined by the CN and NI phase transitions.

its simplicity, proved to be effective provided that appropriate caution is taken for the approximation involved.

In Table 4, the results of the analysis for some monomer LCs such as *n*CBs and *n*OCBs are also included for comparison. The thermodynamic data for the transition of these LCs were taken from the table reported by Orwoll et al.[39] In the monomer LCs, the ratios of $(\Delta S_{NI})_V/(\Delta S_{NI})_P$ for the NI transition are 10−30%, being much smaller than those of the dimers and trimers.

5. Discussion

The nematic conformation of the oxyethylene spacer has been previously investigated. ^{2}H NMR measurements were performed on main-chain dimers (named BuBE-*x*) and polymer liquid crystals having deuterated oxyethylene spacers $-(OCD_2\text{-}CD_2)_xO-$ ($x = 2, 3$) in the bulk nematic state as well as in solution with a nematic solvent, paraoxyazoxyanisol (PAA).[24] In these analyses, the ratio of the deuterium quadrupolar splittings $\Delta\nu/\Delta\nu^R$ ($\Delta\nu$ = spacer, $\Delta\nu^R$ = mesogenic unit) was found to remain nearly invariant over a wide range of temperature and concentration in the LC state. The results obtained are consistent with the previous conclusion drawn on a series of main-chain LC oligomers and polymers comprising α,ω-dialkoxyalkane spacers $-O(CH_2)_nO-$ ($n = 9, 10$).[17−21] As revealed by the ^{2}H NMR studies,[25] the orientational characteristics of the mesogenic units are essentially the same for MBBE-6 and BuBE-*x*, indicating that the nematic conformation of the oxyethylene spacer involved in these LC compounds should also be similar. In the previous work,[17] we have further performed the rotational isomeric state analysis on the ^{2}H NMR data of CBA-9 and -10. The conformational entropy changes ΔS^{conf} thus calculated were favorably compared with the observed values of $(\Delta S_{tr})_V$. Since trimers CBA-T*n* involve two spacers, the values of $(\Delta S_{tr})_V$ were found to be nearly twice of those of the corresponding CBA-*n*'s (cf. Tables 2 and 3). Results of the conformational analysis suggest that similar arguments apply to the phase behaviors of MBBE-6.[25] The concept of the nematic phase described above is schematically illustrated in Figure 7. The conformational ordering of chain segments in the nematic state has also been investigated by other research groups.[40−46] Although molecular constitutions are divergent, the results reported are more or less mutually consistent.

As discussed critically by several authors,[47−49] the free energy change at the NI interphase includes two contributions: (1) anisotropic attractive (Maier−Saupe force)[50,51] and (2) repulsive steric interactions (volume exclusion).[52] The conformational ordering of the intervening flexible spacer at the phase transition may enhance the latter contribution. In our previous dipole moment and optical anisotropy studies on CBA-*n* ($n = 9$ and 10),[16] the optical anisotropies $\langle\gamma^2\rangle$ has been estimated for the nematic configuration of molecules both with and without contribution from the spacer segments. The increments in $\langle\gamma^2\rangle$ due to the nematic arrangements of the flexible spacer were respectively found to be 6.8 and 4.7% for these two LCs. Accordingly, it has been concluded that the spacer should not much contribute to the attractive interactions under the nematic order.[16]

In the thermodynamic treatment of conventional monomer LCs, the contribution from the volume change ΔV_{NI} at the isotropization point is often neglected. The relative volume change $(\Delta V/V)_{NI}$ at the NI transition point is 0.0046 for MBBE-6, being comparable to those estimated for monomer LCs (cf. Table 4): 5CB (0.0043),[39] 7CB (0.0058),[39] 5OCB (0.0030),[39] 8OCB (0.0043),[39] PAA (0.0032),[53] and MBBA (0.0011).[54] Substantially enhanced ratios are obtained for the dimer and trimer carrying α,ω-dialkoxyalkane spacers (cf. Table 3); CBA-9 (0.015),[17] CBA-10 (0.017),[17] CBA-T9 (0.014),[20] and CBA-T10 (0.023).[20] As stated above, the oxyethylene spacer should tend to be more disordered than the α,ω-dialkoxyalkane spacer in the nematic phase. This may provide the reason why the volume change $(\Delta V/V)_{NI}$ of MBBE-6 is smaller relative to those of CBA-*n* and CBA-T*n*.

The $\alpha-T$ relation shown in Figure 4a indicates a discrete change of α at the CN and NI phase boundaries. The value of α ($0.60_3 \times 10^{-3}$ K^{-1}) extrapolated to T_{NI} from the high-temperature I phase is lower than the corresponding value ($0.83_5 \times 10^{-3}$ K^{-1}) obtained from the low-temperature N phase. The trend is opposite for the CN transition. Similar discordance in α at the NI interphase is also observed, but less markedly, for conventional monomer LCs.[53] As pointed out in various thermodynamic theories, α is closely related to the free volume of the liquid.[55,56] The discrete enhancement in α on crossing the NI border from the I phase (i.e., on cooling) may suggest a mechanism such that steric constraints due to the excluded volume effect are alleviated by the spatial rearrangement of mesogenic cores, and the associated ordering of the flexible spacer gives rise to an increase in the free volume. These considerations provide a plausible explanation for the observation that while the macroscopic volume diminishes at the transition, the constituent molecules gain more free volumes. A similar increase in the isothermal compressibility β on the I to N transformation would perhaps arise from the same origin (Figure 4b). Contrary to α and β, the γ value defined as the ratio α/β tends to decrease with raising temperature in all three phases and exhibits a discontinuous reduction at both CN and NI boundaries (cf. Figure 4c).

Recently we have attempted a van der Waals potential analysis on the *PVT* data of MBBE-6 observed in both the isotropic and anisotropic LC state.[57] Assuming the intermolecular interaction potential $E = -\eta/V^m$, the mean-field parameter representing the strength of the interaction field η was estimated by using the relation

$$(\delta E/\delta V)_T = T\gamma - P = m\eta/V^{m+1} \tag{3}$$

Under an atmospheric pressure (i.e., $P \cong 0$)

$$\ln T\gamma = -(m+1)\ln V + \ln m\eta \tag{4}$$

With $m = 1$, the value of η was found to decrease gradually with descending temperature in the isotropic phase until the NI transition emerges. At this point, η exhibits a discrete jump from 2.9×10^{-2} to 3.4×10^{-2} J cm^3 g^{-2}, followed by a decrease with descending temperature over the nematic phase. The increment in η, and thus in E, amounts to ∼13% at the NI boundary. Separate estimates of the contribution due to the rigid

aromatic mesogen and flexible oxyethylene segment are difficult at this moment. The change in η should represent at least partially the variation of the local structure of liquids. Finally, the discontinuities observed in the temperature dependence of α, β, and E at T_{NI} may be mutually related.

6. Concluding Remarks

The odd−even oscillation of thermodynamic quantities at T_{NI} with the parity of the number of spacer atoms has been a subject of many investigations.[58,59] The effect of the linking group X has been examined in our previous work for dimers such as NC$\phi\phi$X(CH$_2$)$_n$X$\phi\phi$CN with $n = 9$ and 10.[14] While the effect was found to be pronounced with X = ester −OC(O)− or ether −O−, it was largely suppressed with X = carbonate −OC(O)O−. The difference was attributed to the disorientation angle (>X) defined by the mesogenic axis and the first bond of the flexible spacer. As shown for a series of MBBE-*x*, the odd−even phenomenon is very weak even with X = ether when oxyethylene-type spacers are used. The odd−even trend characteristic of the tetrahedrally bonded chain system is smeared out by the conformational disordering due to the gauche preference around the OC−CO bond.

As well-known, the orientation-dependent attractive interactions are the most important driving force to form liquid crystalline phase.[50,51] The flexible chain segments inevitably take a one-dimensional nematic order. In principle, therefore, the transition entropy after corrected for the volume change at the I/N boundary must include the contribution from this source in addition to the conformational entropy change due to the flexible spacer ΔS^{conf}:

$$(\Delta S_{tr})_V = \Delta S_{orient} + \Delta S^{conf} \quad (5)$$

where ΔS_{orient} designates the orientational entropy change.[4] As stated above, however, the latter term is overwhelmingly responsible for the constant-volume transition entropy $(\Delta S_{tr})_V$,[17] indicating that contribution from ΔS_{orient} is relatively minor. In this regard, the major contributors of the transition entropies of dimers and higher analogues are quite different from those of conventional monomeric LC compounds.[60,61] Since the NI phase transition takes place between the two fluid states, the obscure contribution from the so-called communal entropy can be safely ignored.[31,36]

As has been demonstrated by careful examinations,[2,17,18,20] the nematic conformation and its thermodynamic characteristics remain nearly invariant for DP ≥ 2 as long as the chemical structure of the spacer is identical. Studies on a dimer model compound provide a good insight for the nematic conformation of flexible chains involved in mesogenic-unit-containing polymers. We would like to emphasize that the thermodynamic role of the spacer elucidated for MBBE-6 (cf. Figure 7) should also be valid for higher homologues including polymer LCs.

Acknowledgment. This work was partially supported by the Private University Frontier Research Center Program sponsored by the Ministry of Education, Culture, Sports, Science and Technology (Monbukagakusho) and also by a Grant-in-Aid for Science Research (18550111) of Monbukagakusho. Z.Z. expresses his gratitude for the Postdoctoral Fellowship for Foreign Researchers sponsored by the Japan Society for the Promotion of Science (JSPS), and he also thanks the support by a Grant-in-Aid for Science Research (P01094) of Monbukagakusho.

References and Notes

(1) Abe, A.; Furuya, H.; Zhou, Z.; Hiejima, T. *Adv. Polym. Sci.* **2005**, *181*, 121−152.
(2) The molecular weight dependence of the transition entropy $(\Delta S_{NI})_P$ has been studied by Blumstein et al.[3] for main-chain LC polymers, DDA-9. When the unit is expressed by the entropy change per spacer, the magnitude of $(\Delta S_{NI})_P$ becomes nearly invariant over a wide range from the dimer model compound (9-DDA-9) to polymers. These results strongly suggest that the spatial configuration of the flexible spacer and its thermodynamic role remain nearly identical independent of the degree of polymerization (DP). The study[3] indicates that the DP dependence of physical properties should be most distinct in the oligomer region.
(3) Blumstein, R. B.; Stickles, E. M.; Gauthier, M. M.; Blumstein, A.; Volino, F. *Macromolecules* **1984**, *17*, 177−183.
(4) Abe, A. *Macromolecules* **1984**, *17*, 2280−2287.
(5) Abe, A.; Furuya, H. *Polym. Bull. (Berlin)* **1988**, *19*, 403−407.
(6) Abe, A.; Furuya, H. *Polym. Bull. (Berlin)* **1988**, *20*, 467−470.
(7) Abe, A.; Furuya, H. *Macromolecules* **1989**, *22*, 2982−2987.
(8) Abe, A.; Shimizu, R. N.; Furuya, H. In *Ordering in Macromolecular Systems*; Teramoto, A., Kobayashi, M., Norisuye, T., Eds.; Springer-Verlag: Heidelberg, 1994; pp 139−153.
(9) Abe, A. *Macromol. Symp.* **1997**, *118*, 23−32 and references cited therein.
(10) Furuya, H.; Dries, T.; Fuhrmann, K.; Abe, A.; Ballauff, M.; Fischer, E. W. *Macromolecules* **1990**, *23*, 4122−4126.
(11) Furuya, H.; Abe, A.; Fuhrmann, K.; Ballauff, M.; Fischer, E. W. *Macromolecules* **1991**, *24*, 2999−3003.
(12) Shimizu, R. N.; Kurosu, H.; Ando, I.; Abe, A.; Furuya, H.; Koroki, S. *Polym. J.* **1997**, *29*, 598−602.
(13) Shimizu, R. N.; Asakura, N.; Ando, I.; Abe, A.; Furuya, H. *Magn. Reson. Chem.* **1998**, *36*, S195−S199.
(14) Furuya, H.; Asahi, K.; Abe, A. *Polym. J.* **1986**, *18*, 779−782.
(15) Abe, A.; Furuya, H.; Nam, S.-Y.; Okamoto, S. *Acta Polym.* **1995**, *46*, 437−444.
(16) Furuya, H.; Okamoto, S.; Abe, A.; Petekidis, G.; Fitas, G. *J. Phys. Chem.* **1995**, *99*, 6483−6486.
(17) Abe, A.; Nam, S.-Y. *Macromolecules* **1995**, *28*, 90−95.
(18) Abe, A.; Furuya, H.; Shimizu, R. N.; Nam, S.-Y. *Macromolecules* **1995**, *28*, 96−103.
(19) Maeda, Y.; Furuya, H.; Abe, A. *Liq. Cryst.* **1996**, *21*, 365−371.
(20) Abe, A.; Takeda, T.; Hiejima, T.; Furuya, H. *Polym. J.* **1999**, *31*, 728−734.
(21) Abe, A.; Hiejima, T.; Takeda, T.; Nakafuku, C. *Polymer* **2003**, *44*, 3117−3123.
(22) Tadokoro, H. *Structure of Crystalline Polymers*; Wiley-Interscience: New York, 1979; Chapter 4.
(23) Abe, A.; Furuya, H.; Mitra, M. K.; Hiejima, T. *Theor. Polym. Sci.* **1998**, *8*, 253−258 and references cited therein.
(24) Furuya, H.; Iwanaga, H.; Nakajima, T.; Abe, A. *Macromol. Symp.* **2003**, *192*, 239−250.
(25) Hiejima, T.; Seki, K.; Kobayashi, Y.; Abe, A. *J. Macromol. Sci., Part B: Phys.* **2003**, 431−439.
(26) Kobayashi, Y. Master Thesis, Tokyo Polytechnic University, 2003.
(27) Mandelkern, L. *Crystallization of Polymers*; McGraw-Hill: New York, 1964; Chapter 5.
(28) Mandelkern, L. *Crystallization of Polymers*; Cambridge University Press: Cambridge, 2002; Vol. 1, Chapter 6.
(29) Tsujita, Y.; Nose, T.; Hata, T. *Polym. J.* **1972**, *3*, 587−590.
(30) Tsujita, Y.; Nose, T.; Hata, T. *Polym. J.* **1974**, *6*, 51−55.
(31) Turturro, A.; Bianchi, U. *J. Chem. Phys.* **1975**, *62*, 1668−1673.
(32) Bianchi, U.; Turturro, A. *J. Chem. Phys.* **1976**, *65*, 697−699.
(33) Karasz, F. E.; Couchman, P. R.; Klempner, D. *Macromolecules* **1977**, *10*, 88−89.
(34) Wunderlich, B.; Czornyj, G. *Macromolecules* **1977**, *10*, 906−913.
(35) Naoki, M.; Tomomatsu, T. *Macromolecules* **1980**, *13*, 322−327.
(36) Wurflinger, A. *Colloid Polym. Sci.* **1984**, *262*, 115−118.
(37) Bleha, T. *Polymer* **1985**, *26*, 1638−1642.
(38) Zoller, P.; Walsh, D. *Standard Pressure-Volume-Temperature Data for Polymers*; Technomic Publishing: Lancaster, 1995.
(39) Orwoll, R. A.; Sullivan, V. J.; Campbell, G. C. *Mol. Cryst. Liq. Cryst.* **1987**, *149*, 121−140.
(40) Yoon, D. Y.; Bruckner, S. *Macromolecules* **1985**, *18*, 651−657.
(41) Samulski, E. T. *Faraday Discuss. Chem. Soc.* **1985**, *79*, 7−20.
(42) Yoon, D. Y.; Bruckner, S.; Volksen. W.; Scott. J. C. *Faraday Discuss. Chem. Soc.* **1985**, *79*, 41−53.
(43) Griffin. A. C.; Samulski, E. T. *J. Am. Chem. Soc.* **1985**, *107*, 2975−2976.
(44) Bruckner, S.; Scott, J. C.; Yoon, D. Y.; Griffin, A. C. *Macromolecules* **1985**, *18*, 2709−2713.
(45) Volino, F.; Ratto, J. A.; Galland, D.; Esnault, P.; Dianoux, A. J. *Mol. Cryst. Liq. Cryst.* **1990**, *191*, 123−133.
(46) Sherwood, M. H.; Sigaud, G.; Yoon, D. Y.; Wade, C. G.; Kawasumi, M.; Percec, V. *Mol. Cryst. Liq. Cryst.* **1994**, *254*, 455−468.
(47) Flory, P. J. *Adv. Polym. Sci.* **1984**, *59*, 1−36.

(48) Vertogen, G.; de Jeu, W. H. *Thermotropic Liquid Crystals, Fundamentals*; Springer-Verlag: Berlin, 1988; Part 2-13, pp 245−282.
(49) Chandrasekhar, S. *Liquid Crystals*, 2nd ed.; Cambridge University Press: Cambridge, 1992; Chapter 2, pp 17−84.
(50) Maier, W.; Saupe, A. *Z. Naturforsch.* **1959**, *14A*, 882−889.
(51) Maier, W.; Saupe, A. *Z. Naturforsch.* **1960**, *15A*, 287−292.
(52) Onsager, L. *Ann. N.Y. Acad. Sci.* **1949**, *51*, 627−659.
(53) Stimpfle, R. M.; Orwoll, R. A.; Schott, M. E. *J. Phys. Chem.* **1979**, *83*, 613−617.
(54) Armitage, D.; Price, F. P. *Phys. Rev. A* **1977**, *15*, 2496−2500.
(55) Flory, P. J. *J. Am. Chem. Soc.* **1965**, *87*, 1833−1838.
(56) Simha, R.; Somcynsky, T. *Macromolecules* **1969**, *2*, 342−350.
(57) Abe, A.; Zhou, Z.; Furuya, H. *Polymer* **2005**, *46*, 4368−4372.
(58) Sirigu, A. In *Liquid Crystallinity in Polymers*; Ciferri, A., Ed.; VCH: New York, 1991; pp 261−313.
(59) Imrie, C. T. In *Liquid Crystals II*; Mingos, D. M. P., Ed.; Springer-Verlag: Berlin, 1999; pp 149−192.
(60) Deloche, B.; Cabane, B.; Jerome, D. *Mol. Cryst. Liq. Cryst.* **1971**, *15*, 197−209.
(61) McColl, J. R.; Shih, C. S. *Phys. Rev. Lett.* **1972**, *29*, 85−87.

MA062447J